

Tunable epitaxial growth of magnetoresistive $\text{La}_{2/3}\text{Sr}_{1/3}\text{MnO}_3$ thin films

J. Fontcuberta,^{a)} M. Bibes, and B. Martínez

Institut de Ciència de Materials de Barcelona-CSIC, Bellaterra 08193, Catalunya, Spain

V. Trtik, C. Ferrater, F. Sánchez, and M. Varela

Departament de Física Aplicada i Òptica, Universitat de Barcelona, Diagonal 647, Barcelona 08028, Catalunya, Spain

We report on the growth of epitaxial $\text{La}_{2/3}\text{Sr}_{1/3}\text{MnO}_3$ thin films on buffered Si(001) substrates. We show that a suitable choice of the buffer heterostructure allows one to obtain epitaxial (00*h*), (0*hh*), and (*hhh*) manganite thin films. The magnetotransport properties are investigated and we have found that the low-field magnetoresistance is directly related to the width of the normal-to-plane rocking curves, irrespective of the film orientation. The magnetic anisotropy of these films has also been determined. © 1999 American Institute of Physics.

[S0021-8979(99)35108-2]

INTRODUCTION

There is a great deal of interest in ferromagnetic manganese perovskites for a number of spin-dependent transport devices. In this regard, the structure of interfaces and its associated resistance are an issue of major concern since they determine low-field magnetotransport response.¹⁻³ A convenient strategy to this objective is the epitaxial growth of $\text{L}_{1-x}\text{A}_x\text{MnO}_3$ (L is a lanthanide and A a divalent alkaline earth) with different orientations. An obvious further advantage for technological applications would be the use of silicon substrates. The growth of manganite films on Si (or on Si with a thermal oxide) substrates faces the difficulty of Si interdiffusion and thermal expansion mismatch.⁴ The recent report of epitaxial growth of SrTiO_3 (00*h*), (0*hh*), or (*hhh*) on buffered Si(001) (Ref. 5) is of particular relevance because SrTiO_3 is an almost ideal substrate for the epitaxial growth of manganite films.

In this article we will take advantage of these results and we will explore the growth of $\text{La}_{2/3}\text{Sr}_{1/3}\text{MnO}_3$ (LSMO) epitaxial thin film on buffered Si(001) substrates using a pulsed laser deposition technique. For all LSMO thin films the uppermost buffer layer is SrTiO_3 (STO) which, with appropriate selection of the underlying buffer layers, can be textured differently, thus allowing one to grow epitaxial $\text{La}_{2/3}\text{Sr}_{1/3}\text{MnO}_3$ films having (001), (011) or (111) orientations.

EXPERIMENT

LSMO thin films and the necessary buffers have been prepared on Si(001) substrates by pulsed laser deposition (PLD) using a KrF excimer laser. The heterostructures of the buffers used are STO/CeO₂/YSZ, STO/YSZ, and STO/TiN/YSZ. These allow tailoring of the texture of the LSMO film. We recall that the following epitaxial relations have been observed: (001)STO[100]//(001)Si[110], (011)STO[01-1]//(001)Si[100], and (111)STO[1-10]//(001)Si[100].

LSMO layers, typically 100 nm thick, were deposited at a substrate temperature of 750 °C, oxygen pressure of 0.40 mbar, and a laser repetition rate of 10 Hz.

The films' structural quality and epitaxial nature were investigated by a four circle x-ray diffractometer. All the crystallographic planes and directions for LSMO referred to in this work are indexed according to cubic notations. Atomic force microscopy (AFM) was used to observe the film morphology and to estimate the surface roughness. The magnetization and electrical resistivity were measured by a Quantum Design superconducting quantum interference device (SQUID) system in the 10–350 K temperature range and under fields up to 50 kOe. In the measurements reported the magnetic field is always in the film plane and parallel to the current.

RESULTS

The x-ray θ - 2θ diffraction patterns of the LSMO/STO/CeO₂/YSZ/Si, LSMO/STO/YSZ/Si, and LSMO/STO/TiN/YSZ/Si thin films show the (00*h*), (0*hh*), and (*hhh*) peaks of the LSMO films indicating the perpendicular-to-the-plane texture of the corresponding films. Thus these films will be labeled (001) LSMO, (011) LSMO, and (111) LSMO. In Fig. 1 we show the θ - 2θ pattern corresponding to (001) and (111) LSMO, i.e., LSMO/STO/CeO₂/YSZ/Si and LSMO/STO/TiN/YSZ/Si, respectively. To the best of our knowledge this is the first report of epitaxial growth of (011) and (111) LSMO films on buffered Si(001) substrates.

The rocking curves are found to increase [full width at half maximum FWHM] from 1.1°, to 1.3°, to 2.4° for the (001), (011), and (111) LSMO films, respectively. These can be compared with the corresponding rocking curves measured for the underlying (001), (011), and (111) STO buffers: 1.3°, 1.5°, and 2.4°, respectively,⁵ thus showing that the quality of the perpendicular texture of the LSMO films essentially mimics that of the STO buffers.

The ϕ scans of the (001) LSMO film, shown in Fig. 2, reveal the existence of a set of reflections which correspond to the family of (301) planes of the LSMO and STO films.

^{a)}Electronic mail: fontcuberta@icmab.es

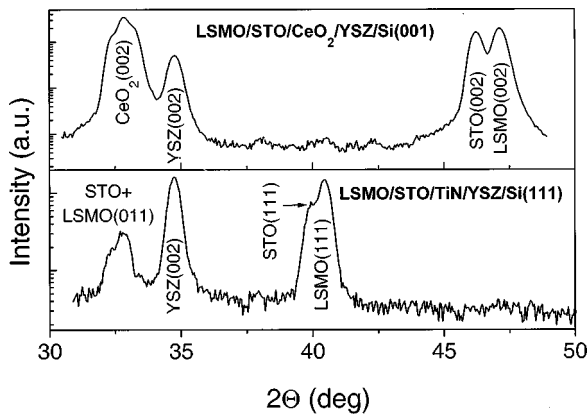


FIG. 1. X ray, θ - 2θ pattern of (001) and (111) LSMO, i.e., LSMO/STO/CeO₂/YSZ/Si and LSMO/STO/TiN/YSZ/Si heterostructures.

This picture reveals a complete in-plane texture and shows that the LSMO layer grows, cube on cube, epitaxially on the SrTiO₃ buffer film. That means that $[hkl]$ directions of LSMO and STO are parallel. The ϕ scans of the (011) plane of the (111) LSMO films show the presence of four sets of three reflections, which reveal the complete in-plane texture.

The roughness of the (001) LSMO film, determined from AFM measurements in a $1\ \mu\text{m} \times 1\ \mu\text{m}$ scan area, is about 5 nm, that is, about one order of magnitude larger than

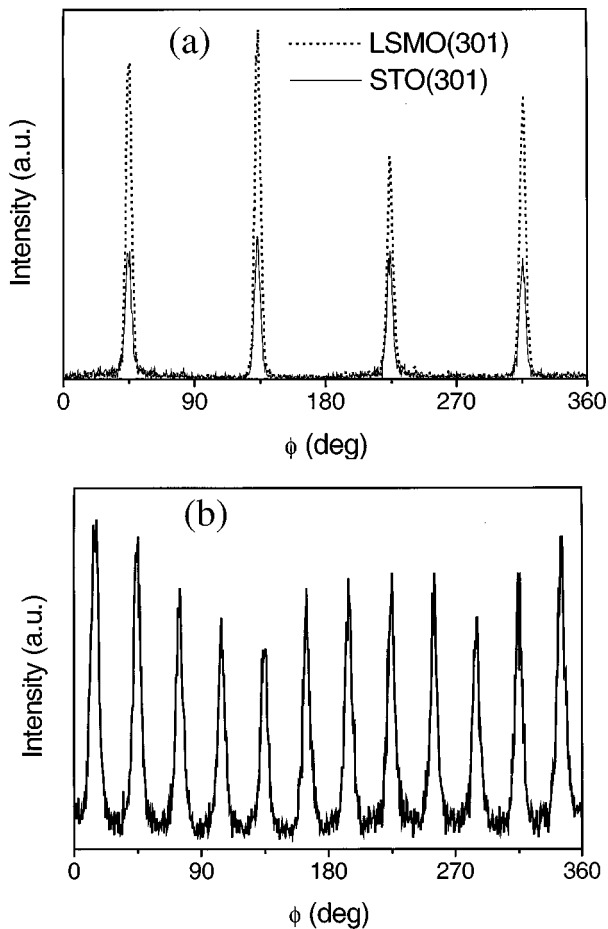


FIG. 2. ϕ scans (a) along the [301] direction of the (001) LSMO film and (b) along the [101] direction of the (111) LSMO film.

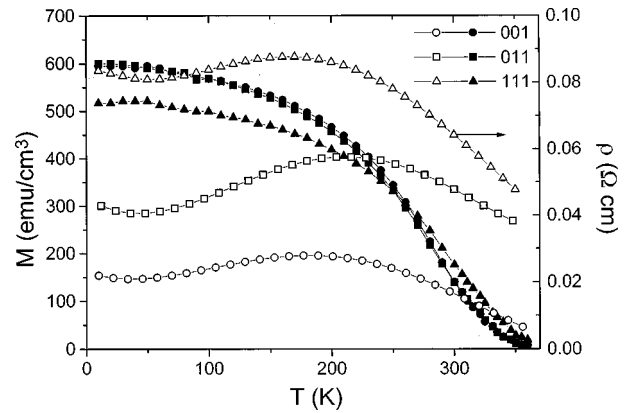


FIG. 3. Temperature dependent magnetization $M(T)$, recorded at 10 kOe, (left side) and zero-field resistivity (right side) for the (001), (011), and (111) films.

that of the underlying STO buffer ($\approx 0.5\ \text{nm}$),⁵ with an average grain size of about 100 nm. We note that the particle size is similar to that observed ($\approx 70\ \text{nm}$) in LSMO films grown by laser ablation on STO single crystals.⁶ Although some prominent pyramidal-shaped particles are visible in the (111) LSMO films, no significant differences in the average roughness and grain size are observed.

The temperature dependent magnetization $M(T)$, recorded at 10 kOe, for these films is shown in Fig. 3. The saturation magnetizations of all films, measured at 10 K, are similar ($\sim 600\ \text{emu/cm}^3$) for the (001) and (011) LSMO and somewhat lower for the (111) LSMO film. There are reports showing that substrate induced stress can substantially modify the magnetization.⁶ However it cannot be excluded that the 10% difference may be due to an enhanced reduction of magnetic ordering at the interfaces in crystallites of (111) LSMO film. In fact, studies on bulk ceramics⁷ and thin films support⁸ this hypothesis. On the other hand, the Curie temperature (T_C) of all films, defined by the sudden rise of magnetization, is about 350 K, close to the values reported ($\sim 360\ \text{K}$) for single crystals, thus showing that the bulk of the crystallites have the right stoichiometry and oxygen contents.

In sharp contrast with the $M(T)$, the resistivity $\rho(T)$ of these samples exhibits substantial differences. As shown in Fig. 3 (rightside), the resistivity at any temperature increases when going from (001) to (110) and (111).

We note that the room-temperature resistivity of our (001) LSMO film is significantly larger [$\rho(300\ \text{K}) \approx 10\ \text{m}\Omega\ \text{cm}$] than that of epitaxial (001) LSMO films on single crystalline substrates ($1.3\ \text{m}\Omega\ \text{cm}$).⁹ The resistivities of the (110) and (111) LSMO films are both larger than that of the (001) LSMO film but smaller than the resistivity of films having a c -axis texture but no in-plane epitaxy ($\approx 1\ \Omega\ \text{cm}$).⁹ This observation clearly reveals the important contribution of intergrain resistance to the overall resistivity.

The isothermal magnetoresistance (MR) $\text{MR} = [\rho(H) - \rho(H=0)]/\rho(H=0)$ of both (100) and (111) LSMO films shows an abrupt decrease of resistivity at low fields, in the 500 Oe range, followed by a more gradual high-field magnetoresistance. This behavior is known to occur in LSMO

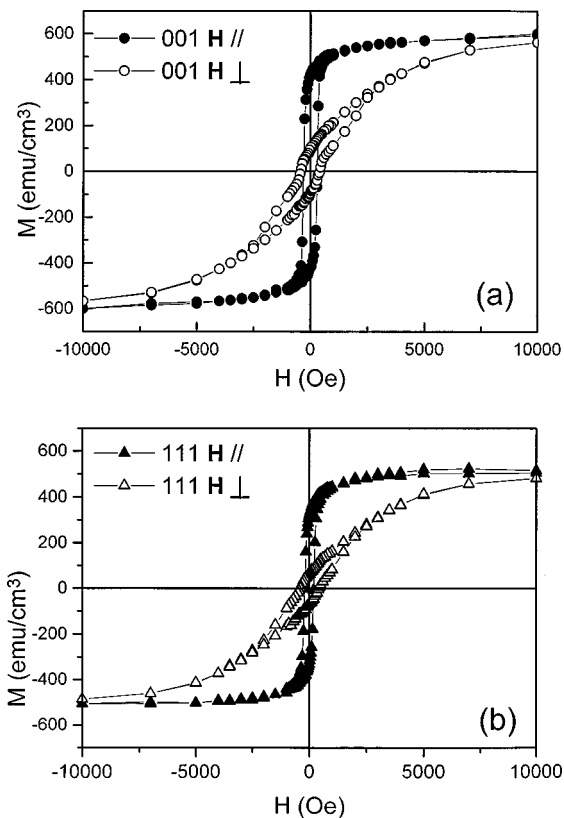


FIG. 4. Magnetization $M(H)$ loops (at 10 K) for the (001) and (111) LSMO films; the \perp and \parallel symbols indicate a measurement with H perpendicular and parallel to the film plane, respectively. LFMR vs the residual resistance ρ (10 K) (bottom axis) and FWHM rocking width ($\Delta\omega$) for (001), (011), and (111) LSMO films. The lines through the data are only guides for the eye.

ceramics and grain boundaries and it has been attributed to interface scattering or the tunneling of carriers. The low-field MR (LFMR), that is, the linear extrapolation of the high-field linear part of $MR(H)$ towards zero field, is in the 10%–20% range and it increases when going from (001) to (011) and (111). This behavior is closely connected to the observed increase of resistivity of these films and should reflect a progressively more prominent contribution by the interfaces in the measured MR. In the inset of Fig. 4(b), where we plot the LFMR versus the residual resistance ρ (10 K), summarizes these findings and reveals the connection between the resistivity and the MR in these films. It also shows the relationship between the LFMR measured and the FWHM ($\Delta\omega$) of the (001), (011), and (111) LSMO rocking curves. Observation of this plot clearly reveals that, for (001) LSMO films, $\Delta\omega$ substantially lower than 1° are required to obtain vanishingly small LFMR values and single crystal-like magnetoresistance behavior. In fact, recent reports of LSMO films on single crystal STO substrates also support this conclusion.⁸ In addition, when comparing the (001), (011), and (111) films, a clear correlation between the normal-to-plane spread directions (and, of course, the in-plane misorientation) and the LFMR can be seen. However, in spite of the substantial differences between the in-plane interfaces of all films, the

LFMR values observed are comparable; the rocking curve $\Delta\omega$ and the corresponding $\Delta\phi$ appear to have a major impact on the magnetoresistance measured, irrespective of the film orientation. This extreme sensitivity of interface magnetoresistance to grain boundaries is not well understood at present.

The hysteresis loops $M(H)$ recorded for all films with the field H perpendicular to the film plane are S shaped as expected for magnetization in the hard direction. On the other hand, when H is parallel to the film plane, the $M(H)$ loops are square, thus indicating that the easy-magnetization axis is in the film plane, irrespective of the film texture. In Fig. 4 we show the $M(H)$ loops, at 10 K, for the (001) and (111) LSMO films. This plot clearly indicates that shape effects dominate the magnetic anisotropy of the films. The same conclusion holds for the (011) LSMO film.

In summary we have shown that epitaxial (00h), (0hh), and (hhh) epitaxial LSMO films on buffered Si(100) substrates can be successfully grown by appropriate selection of a heterostructure buffer layer. Although details of the microstructures of the interfaces in the crystallites are expected to be substantially different for (001), (011), and (111) textured LSMO thin films, the low-field (low-temperature) magnetoresistance measured is found to be comparable, thus suggesting that the spread of normal-to-plane and in-plane axes, as measured by the $\Delta\omega$ and $\Delta\phi$, and the concomitant in-plane induced defects are dominant. It appears that, irrespective of the texturing, shape anisotropy overcomes magnetocrystalline anisotropy.

ACKNOWLEDGMENTS

Financial support by the CICYT (Grant Nos. MAT97-0699 and MAT96-0911) and the CEE OXSEN projects and by the Generalitat de Catalunya (Grant No. GRQ95-8029) are acknowledged.

- ¹H. Y. Hwang, S.-W. Cheong, N. P. Ong, and B. Batlogg, *Phys. Rev. Lett.* **77**, 2041 (1996); J. Fontcuberta, B. Martínez, V. Laukhin, Ll. Balcells, X. Obradors, C. H. Cohenca, and F. Jardim, *Philos. Trans. R. Soc. London, Ser. A* **356**, 1577 (1998).
- ²N. D. Mathur, S. P. Isaac, G. Burnell, B.-S. Teo, L. F. Cohen, J. L. MacManus-Driscoll, J. E. Evetts, and M. G. Blamire, *Nature (London)* **387**, 266 (1997).
- ³K. Steenbeck, T. Eick, K. Kirsh, K. O'Donnell, and E. Steinbeiss, *Appl. Phys. Lett.* **71**, 968 (1997).
- ⁴J. Y. Gu, C. Kwon, M. C. Robson, Z. Trajanovic, K. Ghosh, R. P. Sharma, R. Shreekala, M. Rajeswari, T. Venkatesan, R. Ramesh, and T. W. Noh, *Appl. Phys. Lett.* **70**, 1763 (1997).
- ⁵F. Sánchez, R. Aguiar, V. Trtik, C. Guerrero, C. Ferrater, and M. Varela, *J. Mater. Res.* **13**, 1422 (1998).
- ⁶C. Kwon, M. C. Robson, K.-C. Kim, J. Y. Gu, S. E. Lofland, S. M. Bhagat, Z. Trajanovic, M. Rajeswari, T. Venkatesan, A. R. Kratz, R. D. Gomez, and R. Ramesh, *J. Magn. Mater.* **172**, 229 (1997).
- ⁷Ll. Balcells, J. Fontcuberta, B. Martínez, and X. Obradors, *Phys. Rev. B* **58**, 14697 (1998).
- ⁸B. S. Teo, N. D. Mathur, S. P. Isaac, J. E. Evetts, and M. G. Blamire, *J. Appl. Phys.* **83**, 7157 (1998).
- ⁹J. Y. Gu, S. B. Ogale, M. Rajeswari, T. Venkatesan, R. Ramesh, V. Radmilovic, U. Dahmen, G. Thomas, and T. W. Noh, *Appl. Phys. Lett.* **72**, 1113 (1997).